JCB Article

Central role of α7 nicotinic receptor in differentiation of the stratified squamous epithelium

Juan Arredondo,[1] Vu Thuong Nguyen,[1] Alexander I. Chernyavsky,[1] Dani Bercovich,[2,3] Avi Orr-Urtreger,[4] Wolfgang Kummer,[5] Katrin Lips,[5] Douglas E. Vetter,[6] and Sergei A. Grando[1]

[1]Department of Dermatology, University of California, Davis, Sacramento, CA 95817
[2]Department of Molecular and Human Genetics, Baylor College of Medicine, Houston, TX 77030
[3]Department of Molecular Genetics, Migal-Galilee Technology Center, and [4]Genetic Institute, Tel Aviv Sourasky Medical Center, and Tel Aviv University, 64239 Tel Aviv, Israel
[5]Institut für Anatomie und Zellbiologie, Justus-Liebig-Universität Giessen, Giessen D-35385, Germany
[6]Neuroscience Department, Tufts University, School of Medicine, Boston, MA 02111

Several ganglionic nicotinic acetylcholine receptor (nAChR) types are abundantly expressed in nonneuronal locations, but their functions remain unknown. We found that keratinocyte α7 nAChR controls homeostasis and terminal differentiation of epidermal keratinocytes required for formation of the skin barrier. The effects of functional inactivation of α7 nAChR on keratinocyte cell cycle progression, differentiation, and apoptosis were studied in cell monolayers treated with α-bungarotoxin or antisense oligonucleotides and in the skin of *Acra7* homozygous mice lacking α7 nAChR channels. Elimination of the α7 signaling pathway blocked nicotine-induced influx of $^{45}Ca^{2+}$ and also inhibited terminal differentiation of these cells at the transcriptional and/or translational level. On the other hand, inhibition of the α7 nAChR pathway favored cell cycle progression. In the epidermis of $\alpha7^{-/-}$ mice, the abnormalities in keratinocyte gene expression were associated with phenotypic changes characteristic of delayed epidermal turnover. The lack of α7 was associated with up-regulated expression of the α3 containing nAChR channels that lack α5 subunit, and both homomeric α9- and heteromeric α9α10-made nAChRs. Thus, this study demonstrates that ACh signaling through α7 nAChR channels controls late stages of keratinocyte development in the epidermis by regulating expression of the cell cycle progression, apoptosis, and terminal differentiation genes and that these effects are mediated, at least in part, by alterations in transmembrane Ca^{2+} influx.

Introduction

Recent progress in the identification of genes encoding new members of the neuronal nicotinic acetylcholine receptor (nAChR)* subunit gene superfamily and developing in vivo models for specific subunit gene deletions has revealed that the expression of the acetylcholine (ACh)-gated ion channels is not limited to neurons (Grando, 1997; Lindstrom, 1997). On the other hand, recent results with receptor subunit knockout (KO) mice indicated that certain ganglionic nAChR subtypes are not essential for normal neurological function (Orr-Urtreger et al., 1997; Paylor et al., 1998). These unexpected findings suggested that one of the major biological functions of neuronal-type nAChRs is to subserve trophic, hormone-like effects of ACh in both neuronal and nonneuronal locations. Elucidation of the nonneuronal function of nAChRs, therefore, may lead to better understanding of a complex signaling mechanism mediating interactions of the peripheral nervous system with the surrounding tissues, wherein different cell types use ACh as a common messenger, or a pacemaker.

ACh is a ubiquitous chemical in life that, although is best known for its role in neurotransmission, is produced by practically all types of live cells and is remarkably abundant in the epidermis and other types of the surface epithelium (Grando et al., 1993b; Wessler et al., 1999). It has become evident that ACh can regulate tissue homeostasis in an autocrine and paracrine fashions by exhibiting a plethora of biological effects on different cell types (Wessler et al., 1998).

Address correspondence to Sergei A. Grando, Dept. of Dermatology, University of California, Davis, UC Davis Medical Center, 4860 Y Street, #3400, Sacramento, CA 95817. Tel.: (916) 734-6057. Fax: (916) 734-6793. E-mail: sagrando@ucdavis.edu

*Abbreviations used in this paper: ACh, acetylcholine; AsOs, antisense oligonucleotides; α-BTX, α-bungarotoxin; GAPDH, glyceraldehyde-3-phosphate dehydrogenase; IF, immunofluorescence; KGM, serum-free keratinocyte growth medium; KO, knockout; nAChR, neuronal nicotinic acetylcholine receptor; Nic, nicotine.

Key words: cell cycle; differentiation; α7 acetylcholine receptor; epidermis; knockout mouse

The level of free tissue ACh is controlled by the cholinergic enzymes choline acetyltransferase and acetylcholinesterase that are present in nonneuronal cells lining the cutaneous, respiratory and alimentary tracts, and blood vessels. In these nonneuronal locations, ACh signaling can be mediated by muscarinic and nicotinic receptors. Binding of ACh to the cell membrane receptors elicits several diverse and simultaneous biochemical events, the "biological sum" of which, together with cumulative effects of other hormonal and environmental stimuli, determines a distinct change in the cell cycle.

The nAChRs are classic representatives of the Cys loop superfamily of ligand-gated ion channel proteins or ionotropic receptors, mediating the influx of Na^+ and Ca^{2+} and efflux of K^+ (Steinbach, 1990). The differences in subunit composition of nAChRs determine the functional and pharmacological characteristics of the ion channels formed. 12 nAChR subunit genes encoding a pentameric protein have been identified and designated α2–α10 and three β2–β4, and each subunit has four putative transmembrane-spanning domains (M1–M4) and a similar topological structure. Each of α7, α8, and α9 subunits is capable of forming functional homomeric nAChR channels, which are α-bungarotoxin (α-BTX) sensitive. RT-PCR has amplified α3, α5, α7, α9, α10, β2, and β4 subunits from human keratinocytes (Grando et al., 1995, 1996; Nguyen et al., 2000a, 2001; Sgard et al., 2002), indicating that keratinocytes express both heteromeric and homomeric nAChR channels on their cell membrane. The differences in subunit composition of nAChRs determine the functional and pharmacological characteristics of the ion channels formed.

Current research results indicate that biological effects of ACh in the skin are finely tuned to regulation of each phase of the cell cycle via the intracellular signaling pathways coupled by each particular type of nAChRs (Grando, 1997, 2001). In keratinocytes, nAChRs control cell viability, proliferation, differentiation, adhesion, and motility, and constant stimulation of keratinocyte nAChRs with endogenously secreted ACh produced by these cells is essential for cell survival. We have demonstrated recently that programmed cell death of keratinocytes culminates in apoptotic secretion of a humectant upon secretagogue action of ACh and that activation of ACh signaling through the α7 nAChR, which is predominantly expressed by mature keratinocytes, is essential for a sustained turnover of the epidermis in humans (Nguyen et al., 2001).

This study was designed to ultimately determine the role for α7 nAChR in mediating physiologic control of keratinocyte differentiation by endogenous ACh. Alterations in the nicotinergic regulation of keratinocyte cycle progression, differentiation, and apoptosis were investigated in three independent models of functionally inactivated α7 nAChR: in cultured human keratinocytes treated with α-BTX or antisense oligonucleotides (AsOs) and epidermal keratinocytes grown from and residing in the skin of KO mice with homozygous-null mutation of the gene-encoding α7 nAChR subunit. We found that pharmacological blockage of α7 nAChR with α-BTX inhibits nicotine (Nic)-induced influx of $^{45}Ca^{2+}$ in human keratinocytes, which is associated with an inhibition of Nic-induced terminal differentiation of these cells. Functional inactivation of α7 nAChRs in cultured human keratinocytes with AsOs abolished high extracellular Ca^{2+}-induced up-regulated synthesis of the terminal differentiation proteins. Terminal differentiation gene expression was found to be down-regulated in the epidermis of α7 KO mice whose keratinocytes demonstrated profound alterations in the normal cell cycle progression and apoptosis when grown in culture. The $\alpha7^{-/-}$ keratinocytes also demonstrated changes in the gene expression of α3, α5, α9, and α10 nAChR subunits, suggesting that ACh signaling in these cells is rerouted to alternative nicotinergic pathways.

Results

The α-BTX–sensitive component of nicotinergic control of keratinocyte differentiation

Nicotinergic agents have been demonstrated to affect the rate of keratinocyte differentiation. It has been shown that Nic accelerates the rate of keratinocyte differentiation which can be abolished by mecamylamine (Grando et al., 1996), an antagonist of the "neuronal" types of the nAChRs expressed in epidermal keratinocytes (Grando et al., 1995). Since keratinocytes express both the heteromeric nAChRs containing α3 subunit, which are not sensitive to α-BTX, and the homomeric α7 nAChR, which is highly sensitive to α-BTX (Levandoski et al., 1999), we investigated effects of α-BTX on the Nic-induced keratinocyte differentiation in confluent monolayers of the second passage human foreskin keratinocytes incubated in the medium containing 0.09 mM Ca^{2+}, in which both test drugs were dissolved. As seen in Fig. 1, after 14 d of

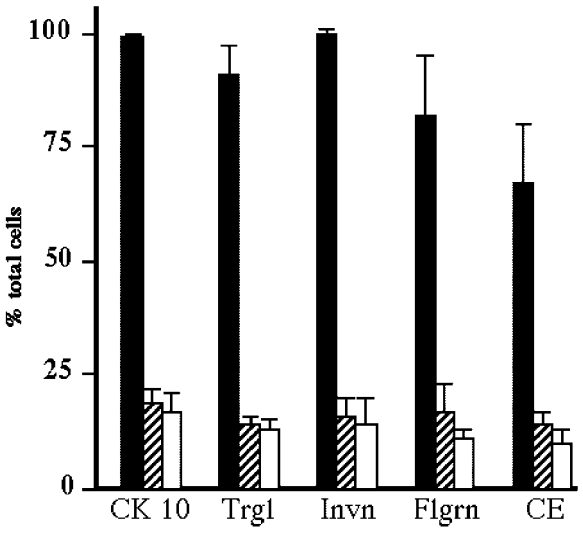

Figure 1. **α-BTX blocks Nic-induced differentiation of human keratinocytes.** The number of differentiation marker-positive keratinocytes (percentage of total cells) after incubation with 10 μM Nic alone (black bar), 10 μM Nic plus 1 μM αBTX (hatched bar), or without any additions (white bar) (control). The cells were either fixed and stained for the differentiation markers cytokeratin 10 (CK 10), human keratinocyte transglutaminase type I (Trgl), involucrin (Invn), or filaggrin (Flgrn) or used in the assay of cornified envelopes (CE). Data are means ± SD of two independent experiments. In each immunocytochemical experiment, the numbers of cells stained for a differentiation-associated protein using avidin–biotin complex/alkaline phosphatase technique (as described in Material and methods) were counted in at least three different microscopic fields.

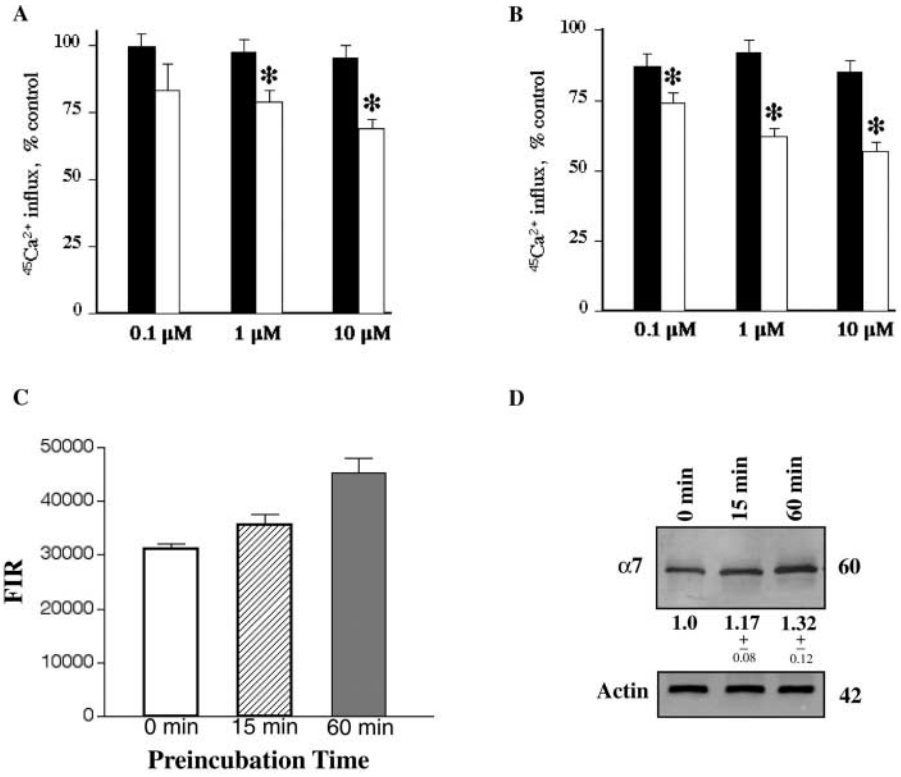

Figure 2. **Role of α7 nAChRs in mediating spontaneous and Nic-induced $^{45}Ca^{2+}$ influx into human keratinocytes.** (A and B) Effects of α-BTX on transmembrane $^{45}Ca^{2+}$ influx. α-BTX decreased in a dose-dependent manner both spontaneous (A) and Nic-induced (B) influx of $^{45}Ca^{2+}$ into keratinocytes freshly isolated from human neonatal foreskins. The effects of test concentrations of α-BTX on baseline $^{45}Ca^{2+}$ influx were measured in cell aliquots suspended in KGM without Nic. The inhibitory effects of α-BTX on Nic-induced $^{45}Ca^{2+}$ influx into keratinocytes were measured in aliquots of keratinocyte suspensions in KGM containing 10 μM Nic. Cell aliquots were resuspended in serum-free keratinocyte medium (KGM) containing either 0.09 (black bar) or 1.2 (white bar) mM Ca^{2+}, incubated for 15 min in a humid 5% CO_2 incubator, washed, and used in the $^{45}Ca^{2+}$ influx assay as described in Materials and methods. Data are means ± SD of representative experiments in which triplicate samples were measured. The concentrations of α-BTX are shown at the bottom of each graph. Asterisks indicate that the experimental data significantly ($P < 0.05$) differ from controls. (C and D) Effects of extracellular Ca^{2+} on expression of α7 nAChR in human keratinocytes. The level of α7 expression on the cell membrane was measured using the FITC-labeled α-BTX binding assay detailed in Materials and methods, and the total amount of cellular α7 protein was measured by Western blotting using rabbit anti-α7 antibody characterized in the past (Zia et al., 2000). Both 15- and 60-min preincubations increased cell surface binding of α-BTX (C). An increase of fluorescence intensity ratio (FIR) became statistically significant after 60 min of incubation ($P < 0.05$; denoted with an asterisk). By this point in time, the total amount of α7 protein increased by 32% (D). The α7 band appeared at the expected mol wt of 60 kD.

exposure to both Nic (10 μM) and α-BTX (1 μM) the number of keratinocytes that stained for the differentiation markers cytokeratin 10, transglutaminase, involucrin, or filaggrin, or spontaneously formed cornified envelopes was significantly ($P < 0.01$) diminished compared with that found in the positive control cultures exposed to 10 μM Nic alone and did not significantly differ from the control values ($P > 0.05$). After shorter incubation periods, i.e., 4, 8, or 10 d, the changes were less pronounced (unpublished data). The cellular staining patterns produced by antibodies to the differentiation markers were similar in experimental and control cultures. Thus, the ability of α-BTX to abolish Nic-induced differentiation of keratinocytes indicated that the differentiation-inducing effect of Nic is predominantly mediated by activation of α7 nAChR.

The α-BTX–sensitive component of the nicotinergic control of transmembrane $^{45}Ca^{2+}$ influx in keratinocytes

Previously, we have shown that Nic increases $^{45}Ca^{2+}$ influx into keratinocytes freshly dissociated from human epidermis, which could be abolished by mecamylamine (Grando et al., 1996). Using the same cell preparation, we tested the effects of α-BTX on $^{45}Ca^{2+}$ influx. The presence of α-BTX in the solution diminished both basal (Fig. 2 A) and Nic (10 μM)-elicited (Fig. 2 B) $^{45}Ca^{2+}$ influx. However, these effects did not reach significant levels at either of three (0.1, 1.0, and 10 μM) α-BTX concentrations tested ($P > 0.05$). Since incubation of keratinocytes in the presence of high extracellular Ca^{2+} up-regulates expression of the gene coding for α7 subunit (Zia et al., 2000), we hypothesized that preincubation of keratinocytes at high (1.2 mM) Ca^{2+} before the $^{45}Ca^{2+}$ influx assay might increase the sensitivity of Nic-elicited $^{45}Ca^{2+}$ influx to a blockage with α-BTX. As expected, in pretreated cells α-BTX inhibited $^{45}Ca^{2+}$ influx in a dose-dependent manner (Fig. 2). To directly address the role of α7-made nAChR channels in mediating these α-BTX effects, we measured effects of short (15 min) and long (60 min) term preincubations at 1.2 mM Ca^{2+} on the relative amount of α-BTX binding to the cell membrane of keratinocytes and total amount of the α7 protein present in these cells, using ELISA with FITC-labeled α-BTX and Western blot with rabbit anti-α7 antibody, respectively. We found that a short term preincubation moderately and a long term preincubation significantly ($P < 0.05$) increased both cell surface expression of α7 nAChR and total amount of the receptor protein in the cells (Fig. 2, C and D). Together, these results indicated that α7-made nicotinic channels may be a major contributor to transmembrane influx of $^{45}Ca^{2+}$ in epidermal keratinocytes at increased extracellular Ca^{2+} levels.

α7 AsOs alters terminal differentiation of cultured keratinocytes

Having found that pharmacological inactivation of α7 nAChR with α-BTX abolishes Nic-induced differentiation, we asked if elimination of α7-coupled pathway can block terminal differ-

Table I. **Oligodeoxynucleotides (ODNs) used in this study**

ODN	Sequence	Function
α7.1	5′-(F[a])CGTAAGACCAGGACCAAACTTCAG-3′	Fluorescein ODN α7 antisense
α7.2	5′-C[b]GAGCAGCATGAAGACGGTAA[b]G-3′	Phosphorothioated α7 antisense
α7.3	5′-G[b]GTCCAGAACTACAATCCCT[b]T-3′	Phosphorothioated α7 antisense
α7.4	5′-C[b]CAATGACTCGCAACCACTCA[b]C-3′	Phosphorothioated α7 antisense
α7.5	5′-T[b]CATGGACGTGGATGAGAAGAA[b]C-3′	Phosphorothioated α7 antisense
α7.6	5′-G[b]ACGCCACATTCCACACTAAC[b]G-3′	Phosphorothioated α7 antisense
α7.6	5′-C[b]TGCGGTGTAAGGTGTGATTG[b]C-3′	Phosphorothioated α7 sense

[a]Fluorescein.
[b]Phosphorothioate.

entiation of keratinocytes. To inhibit α7 expression, we used phosphorothioated AsOs targeted to mRNA for the α7 nAChR subunit (Table I). In keratinocytes lacking α7 nAChR, terminal differentiation can be induced via a Nic-independent pathway mediated by other types of Ca^{2+}-permeable ion channels due to increased concentration of extracellular Ca^{2+}. Nuclear AsOs uptake of the FITC-tagged AsOs by keratinocytes was monitored using a fluorescence microscope (Fig. 3 A). Treatment protocol was optimized to allow maximal inhibition, i.e., >80%, as judged from the results of quantitative receptor protein analysis by Western blotting (Fig. 3 B). The specificity of antibody binding to the immunoblotting membranes was confirmed by (a) appearance of α7 protein band at the expected mol wt (Nguyen et al., 2000a) and (b) absence of this band in negative control experiments omitting primary antibody or replacing it with an irrelevant and species- and isotype-matching antibody (unpublished data).

To determine the effect of inhibited α7 nAChR expression on the unfolding of the keratinocyte differentiation program, preconfluent monolayers of human keratinocytes were fed with serum-free keratinocyte growth medium (KGM) containing a differentiation-inducing concentration of Ca^{2+}, 1.2 mM, and incubated in a humid 5% CO_2 incubator at 37°C for 96 h in the presence (experiment) or absence (baseline) of a mixture of five phosphorothioated anti-α7 AsOs or the same concentration of sense oligonucleotide used as a negative control for AsOs (Table I). After incubation, relative amounts of differentiation marker proteins were measured in experimental and control cells and compared. As seen in Fig. 3 C, functional deletion of α7 nAChR

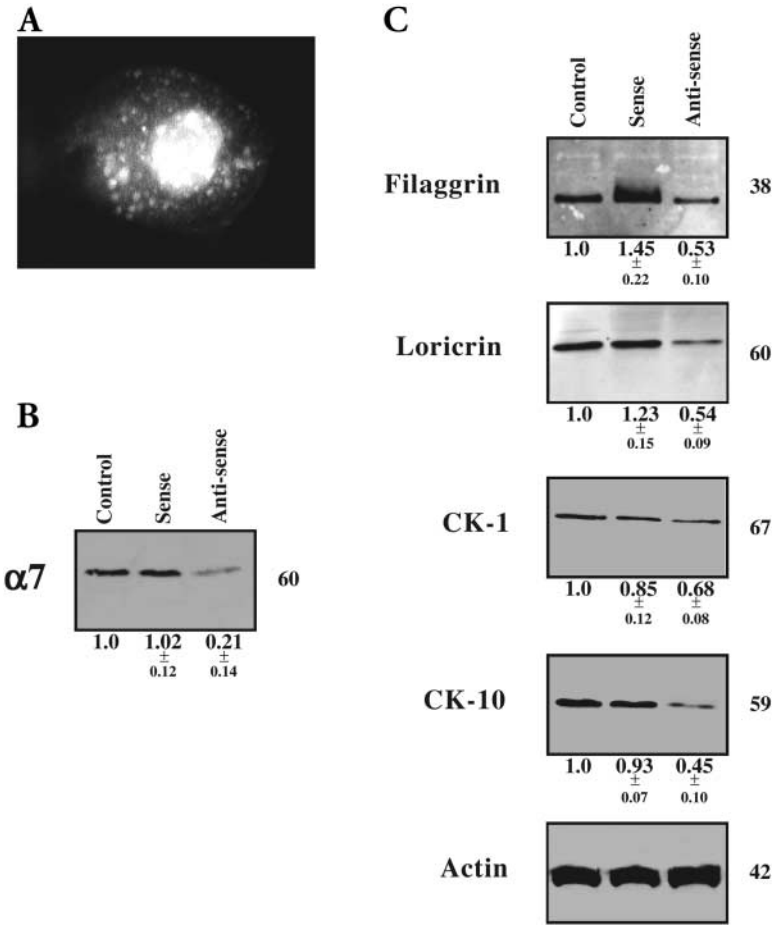

Figure 3. **Anti-α7 AsOs prevents high extracellular Ca^{2+}-induced terminal differentiation of human keratinocytes.** (A) Intracellular accumulation of FITC-labeled α7 AsOs. FITC-labeled AsOs (Table I), 20 nM, was added to the second passage human keratinocytes. Localized FITC-labeled AsOs was viewed live via phase–contrast fluorescence microscopy after a 24-h incubation (×400). Note that anti-α7 AsOs is distributed into the nucleus and the cytoplasm. Control oligonucleotide was similarly distributed (unpublished data). (B) Effect of anti-α7 AsOs on the α7 nAChR subunit protein in human keratinocytes. The cells were seeded in 24-well plates at a density of 5 x 10^4/well and incubated in a 5% CO_2 incubator for 72 h in KGM in the presence of Lipofectamine Plus™ alone (control), 20 nM of sense oligonucleotide, or 20 nM of each of five phosphorothioated AsOs (Table I). The anti-α7 AsOs dramatically reduced the intensity of the 60-kD receptor band in the immunoblot. Control (i.e., sense) oligonucleotide did not alter the total amount of α7 protein. (C) Alterations in the expression of differentiation markers in keratinocytes treated with anti-α7 AsOs. Relative amounts of filaggrin, loricrin, and cytokeratins (CK) 1 and 10 were analyzed by Western blotting of the total protein isolated from human keratinocytes transfected with anti-α7 AsOs or the control oligonucleotide described above, or intact keratinocytes after 96 h incubation of these cells in KGM containing 1.2 mM Ca^{2+}, to induce terminal differentiation.

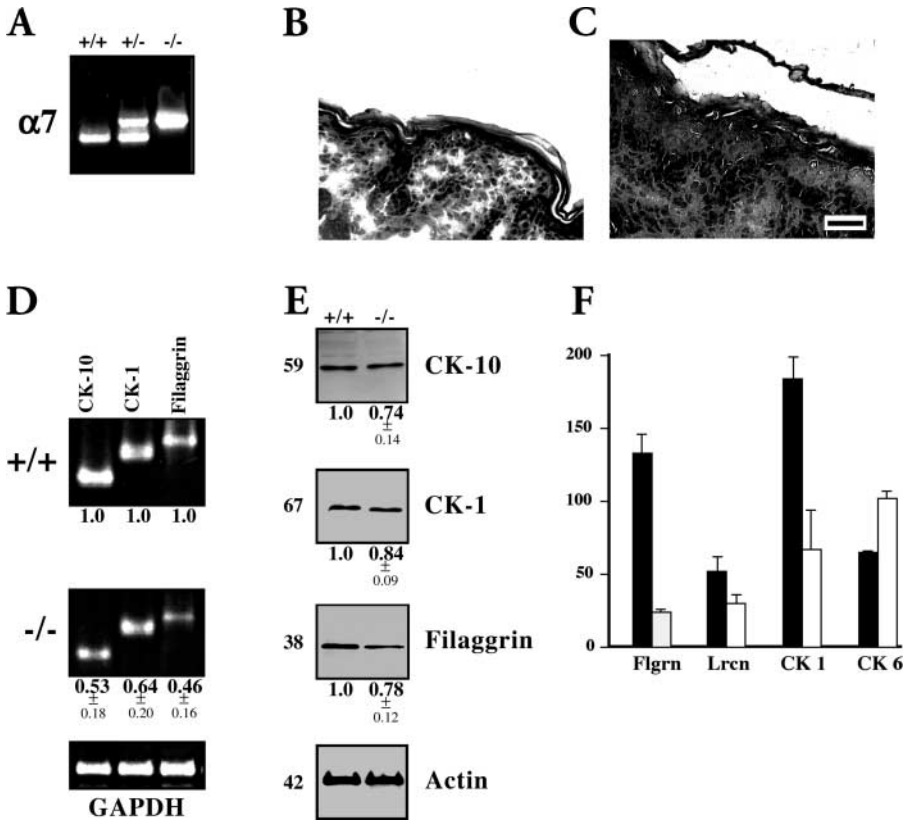

Figure 4. **Reduced rate of keratinocyte cornification in the epidermis of α7 KO mice.** (A) Representative PCR profiles of the homozygous and heterozygous mice from a progeny of a heterozygous $\alpha7^{+/-}$ mouse. Genomic DNA was extracted by a standard digestion method (Orr-Urtreger et al., 1997). The PCR primers were generated for intronic regions flanking exon 8 and 10 and used in experiments at the following concentrations: P1 (wild-type forward), CCTGGTCCTGCT-GTGTTAAACTGCTTC (20 pmol); P2 (wild-type reverse), CTGCTGGGAAATC-CTAGGCACACTTGAG (10 pmol); and P3 (KO), GACAAGACCGGCTTCCATC-CGAGTAC (25 pmol). DMSO (1:20) was included in PCR reactions, and the annealing temperature was 56°C. The size of the gene product amplified from a wild-type mouse was 440 bp and that from $\alpha7^{-/-}$ mouse was 750 bp. The PCR analysis identifies the α7 homozygous-null (−/−) and wild-type (+/+) animals and the heterozygous (+/−) mouse. (B and C) Comparative histology of the skin of $\alpha7^{+/+}$ (B) and $\alpha7^{-/-}$ (C) mice. The epidermis of wild-type mouse is comprised of basal keratinocytes attached to the epidermal basal membrane and a single suprabasal cell layer. In marked contrast, the epidermis of $\alpha7^{-/-}$ mouse, in addition to the basal layer, consists of several rows of suprabasal keratinocytes, including a superficially located layer of granular keratinocytes, and the uppermost stratum corneum, which is unusually loose and thick. Light microscopy of the hematoxylin and eosin stained 6-μm-thick cryostat sections of skin obtained from heads of 3-d-old $\alpha7^{+/+}$ and $\alpha7^{-/-}$ mice. Magnification, ×200. Bar, 25 μm. (D) Analysis of the expression of keratinocyte differentiation proteins cytokeratin (CK) 1, CK 10, and filaggrin by RT-PCR. The mRNA levels of the keratinocyte differentiation markers were determined using specific PCR primers (Table II) and cDNA template from the skin of neonatal α7 KO and wild-type mice as described in Materials and methods. Amplification yielded PCR products of the expected sizes: 534 bp for filaggrin, 461 bp for CK 1, and 364 bp for CK 10. Amplification of the GAPDH gene product (354 bp) was used to normalize the cDNA content in each sample and as a positive control for RT-PCR effectiveness. (E) Analysis of the expression of keratinocyte differentiation proteins CK 1 and 10 and filaggrin by Western blotting. These markers of terminal differentiation were visualized at the expected mol wt (shown in kD on the left side of the gels) in the 15% SDS-PAGE–resolved proteins, 10 μg per lane, extracted from the skin of α7 KO and wild-type mice using specific antibodies, and all appropriate negative controls. (F) Semiquantitative IF analysis of relative amounts of differentiation markers in the epidermis of α7 KO and wild-type neonatal mice. The cryostat sections of the skin from killed mice were stained with antibodies specific for the keratohyalin granule proteins filaggrin (Flgrn), and loricrin (Lrcn), and the CK proteins 1 and 6 (Table III), and the relative amounts of these keratinocyte proteins in the epidermis of $\alpha7^{+/+}$ (black bar) and $\alpha7^{-/-}$ (white bar) mice were determined using computer-assisted analyses of the specific IF tissue staining as detailed in the Materials and methods section. The assay revealed that although the expression of filaggrin, loricrin, and CK 1 was significantly decreased, that of CK 6 was significantly increased in $\alpha7^{-/-}$ compared with $\alpha7^{+/+}$ mice ($P < 0.05$).

resulted in characteristic changes in the differentiation gene expression. We found an ~50% decrease of the levels of filaggrin, loricrin, and cytokeratins 1 and 10, compared with the levels found in control, nonexposed cells. This effect of anti-α7 AsOs markedly differed from that of the control (sense) oligonucleotide, which produced only minor fluctuations of the protein levels of the differentiation markers under consideration (Fig. 3 C). Thus, α7 AsOs-treated keratinocytes showed resistance to Ca^{2+}-induced cornification. These results indicated that inactivation of the α7 nAChR-coupled pathway of ACh signaling interferes with terminal differentiation of human keratinocytes.

Abnormal keratinocyte differentiation in the skin of α7 KO mice

To correlate changes in the cell cycle and differentiation gene expression resulting from inactivation of α7 nAChR-coupled signaling pathways in vitro with the in vivo phenotype caused by the absence α7 nAChR channels in the epidermis, we studied pups delivered by $\alpha7^{+/-}$ mice, followed by genotyping (Fig. 4 A). Compared with wild-type $\alpha7^{+/+}$ mice aged from 1 to 3 wk, whose epidermis usually consists of one to two rows of live nucleated keratinocytes and a compact horny layer comprised of dead corneocytes (Fig. 4 B), $\alpha7^{-/-}$ mice featured thickened, multilayered epidermis (Fig. 4 C). In addition to the lowermost basal layer, the epidermis in $\alpha7^{-/-}$ mice contained an additional two to three suprabasilar rows of pale and enlarged keratinocytes and from one to three rows of granular keratinocytes located just below widened and loose horny layer. Thus, the phenotypic abnormalities in the epidermis of α7 KO mice were consistent with retention hyperkeratosis, which is a morphologic manifestation of delayed epidermal turnover.

To relate changes in the skin development of α7 KO mice to α7 nAChR-mediated control of keratinocyte cell cycle

Table II. **Murine genes studied by RT-PCR**

Common name	Abbreviation	Gene name	Accession no.[a]	Primers
Glyceraldehyde-3-phosphate dehydrogenase	Gapdh	*Gapd*	M17701	214–234, 401–449
nAChRs				
Subunit α3	α3	*Chrna3*	XO3440	434–455, 895–918
Subunit α5	α5	*Chrna5*	AF204689	788–801, 1,238–1,257
Subunit α7	α7	*Chrna7*	AF225980	555–575, 1,027–1,048
Subunit α9	α9	*Chrna9*	AK010496	385–406, 821–842
Subunit α10	α10	*Chrna10*	NM022639	340–358, 720–742
Cell cycle markers				
p53-dependent G2 arrest	p53	*Reprimo*	AB043586	94–118, 463–482
Proliferation-related Ki-67antigen	Ki-67	*Mki67*	X82786	1,091–1,113, 1,570–1,589
Proliferation cell nuclear antigen	PCNA	*Pcna*	X57800	131–150, 437–415
Cyclin D1	Cyl 1	*Ccnd1*	M64403	339–369, 797–820
Cell differentiation markers				
Cytokeratin 1	CK1	*Krt1*	M27734	307–330, 744–767
Cytokeratin 10	CK10	*Krt10*	V00830	202–225, 665–642
Filaggrin		*Flg*	J03458	278–298, 588–609
Cell apoptosis markers				
Bcl-2, apoptosis inhibitor	Bcl-2	*Bcl2*	L31532	376–399, 730–751
Caspase 3, apoptosis-related cysteine protease	CPP32	*Casp3*	U54801	225–246, 657–676

[a]Sequence data available from GenBank/EMBL/DDBJ.

and differentiation, we performed quantitative analysis of mRNA and protein levels of the genes encoding keratinocyte differentiation markers in α7 KO compared with wild-type $\alpha7^{+/+}$ mice. Gene-specific primers for murine filaggrin and cytokeratins 1 and 10 (Table II) amplified products of the expected sizes (Fig. 4 D). The *Acra7* homozygous mutant mice showed decreased mRNA levels of all three terminal differentiation markers, ranging from 36 to 54%. The glyceraldehyde-3-phosphate dehydrogenase (GAPDH) gene amplification remained constant in each experiment (Fig. 4 D).

Findings of down-regulated expression of terminal differentiation genes in keratinocytes residing in the epidermis of $\alpha7^{-/-}$ mice were corroborated by results of the Western blot assay (Fig. 4 E). The α7 deletion was associated with the decrease of the filaggrin and cytokeratin 1 and 10 proteins.

To ultimately determine changes in the differentiation proteins in epidermis of α7 KO mice, we measured the relative intensities of specific staining of keratinocytes produced by antibodies against the keratohyaline proteins filaggrin and loricrin and the intermediate filament proteins cytokeratin 1 and 6, using semiquantitative immunofluorescence (IF) assay. We found that in the epidermis of $\alpha7^{-/-}$ mice, the abundance of terminally differentiated keratinocytes expressing filaggrin, loricrin, and cytokeratin 1 was significantly ($P < 0.05$) less than that in the epidermis of $\alpha7^{+/+}$ mice (Fig. 4 F). In marked contrast, the intensity of epidermal staining for cytokeratin 6, a marker of rapidly proliferating, immature keratinocytes (Foley et al., 1998; Gibbs et al., 2000), was significantly increased ($P < 0.05$), which is consistent with the appearance of the prolonged epidermal turnover phenotype in $\alpha7^{-/-}$ mice.

Abnormalities in cell cycle regulation of α7 KO keratinocytes

When cell cycle and apoptosis gene expression in $\alpha7^{-/-}$ keratinocytes was analyzed by RT-PCR, we found that Ki-67, cyclin D1, and PCNA were increased by 52, 77, and 52%, respectively, compared with $\alpha7^{+/+}$ cells (Fig. 5 A). The mRNA level of p53 also increased by 54%. By immunoblotting, we found that the relative amount of Ki-67, cyclin D1, PCNA, and p53 were increased in $\alpha7^{-/-}$ keratinocytes (Fig. 5 B). On the other hand, the mRNA and protein levels of caspase-3 decreased 24 and 57%, respectively, whereas those of Bcl-2 both increased (Fig. 5).

The results of the semiquantitative IF assay confirmed the above findings (Fig. 5 C). As expected from the results of RT-PCR and immunoblotting assays, we found significant ($P < 0.05$) increases of the relative amounts of keratinocyte Ki-67, PCNA, cyclin D1, and p53 and a decrease of caspase 3 in keratinocytes residing in the epidermis of α7 KO mice compared with the epidermis of wild-type mice. These results suggested that in the absence of α7 nAChR, the nicotinergic pathway of autocrine and paracrine control of keratinocyte growth and differentiation is predominantly mediated by other type(s) of ACh-gated ion channels that are coupled to maintenance of the immature cell phenotype.

Altered expressions of nicotinic receptor subunits in α7 KO keratinocytes

To test a hypothesis that mutational deletion of *Acra7* in keratinocytes evokes changes in the relative amounts of different nAChR channels, we investigated expression of the genes coding for α3, α5, α9, and α10 subunits in $\alpha7^{-/-}$ versus $\alpha7^{+/+}$ keratinocytes. By RT-PCR, we found that the expression of the gene coding for α3 in $\alpha7^{-/-}$ keratinocytes was up-regulated by 56%, whereas that of α5 was apparently unchanged (Fig. 6 A). Results of the Western blotting assay showed an 86% increase of the relative amount of α3 protein in $\alpha7^{-/-}$ keratinocytes (Fig. 6 B). The protein level of α5 was found to be unchanged. These results indicated that although the total number of α3 containing nAChR increases in the epidermis of α7 KO mice, the proportion of the α3 nAChRs containing α5 subunit is actually less then in wild-type mice. The relative amounts of both mRNA and proteins of α9 and

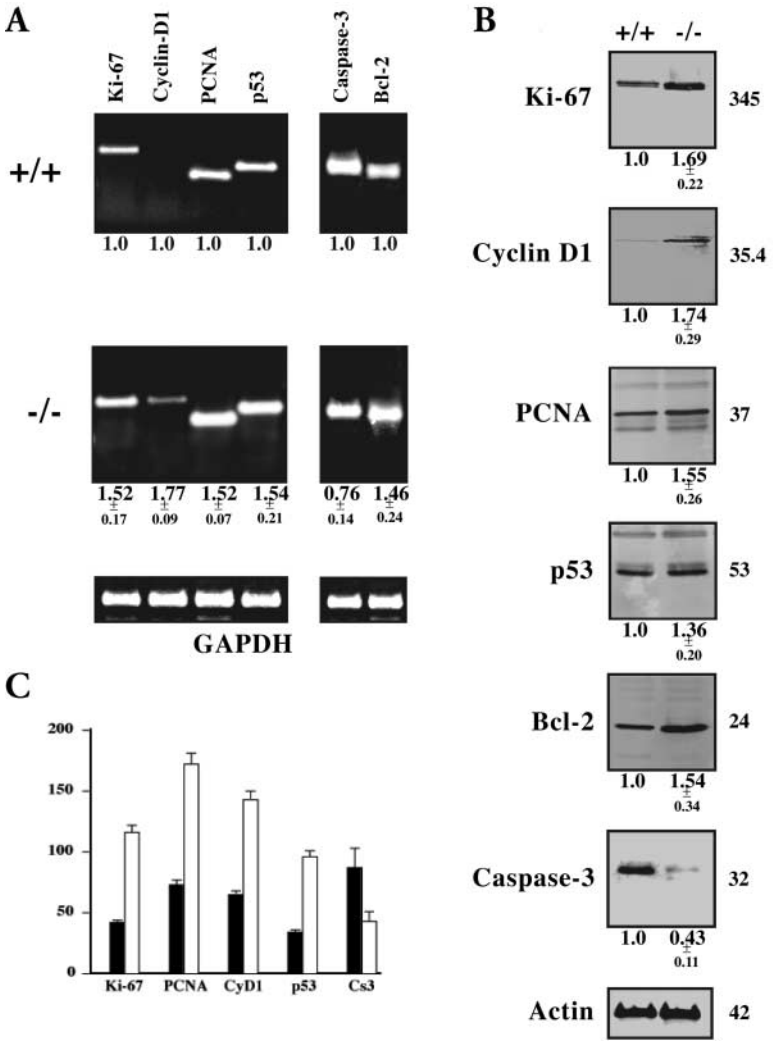

Figure 5. **Alterations in the cell cycle and apoptosis gene expression in α7 KO keratinocytes.** (A) Analysis of the expression of keratinocyte cell cycle and apoptosis regulatory genes by RT-PCR. Total RNA was isolated from the second passage, ~75% confluent monolayers of neonatal α7 homozygous-null (−/−) and wild-type (+/+) keratinocytes and used in the RT-PCR assays described in Materials and methods. Gene-specific RT-PCR primers were designed to amplify the murine cell cycle regulation genes coding for p53, Ki-67, cyclin D1, and PCNA, antiapoptotic Bcl-2, and the cell apoptosis marker gene caspase 3 (Table II). Each primer set yielded PCR product of expected size: 499 bp for Ki-67, 482 bp for cyclin D1, 307 bp for PCNA, 389 bp for p53, 376 bp for Bcl-2, and 494 bp for caspase 3. (B) Analysis of the expression of keratinocyte cell cycle and apoptosis regulatory genes by Western blotting. Total protein was isolated from the same cells as in A and used in the Western blotting assay described in Materials and methods. The mol wt of each protein is shown in kD to the right of the gels. Each protein band was visualized at the expected mol wt. Changes in the gene expression of each of the cell cycle and apoptosis markers detectable by Western blots were consistent with those determined by RT-PCR. (C) Semiquantitative IF analysis of relative amounts of keratinocyte cell cycle and apoptosis markers in the epidermis of α7 KO and wild-type neonatal mice. The cryostat sections of skin from killed mice were stained with antibodies specific for the cell cycle progression regulators Ki-67, PCNA, cyclin D1 (CyD1), and p53, and the marker of cell apoptosis caspase 3 (Cs3) (Table III), and the relative amounts of these keratinocyte proteins in the epidermis of $\alpha7^{+/+}$ (black bar) and $\alpha7^{-/-}$ (white bar) mice were computed based on the relative intensity of specific IF staining as detailed in Materials and methods.

α10 subunits were elevated in $\alpha7^{-/-}$ keratinocytes (Fig. 6). However, an increase of the protein level of α9 by 63% exceeded that of α10 subunit, indicating that both the heteromeric α9α10 and the homomeric α9-made ACh-gated ion channels were up-regulated in $\alpha7^{-/-}$ keratinocytes.

Discussion

This study provides several lines of evidence that the α7 nAChR-mediated signaling is critical for normal epidermal differentiation. We used three independent approaches to inhibit this nicotinergic pathway of ACh signaling in keratinocytes and consistently identified reciprocal changes in the expression of the cell cycle progression and differentiation regulators. The keratinocytes treated with α-BTX or a mixture of phosphorothioated AsOs targeted to mRNA for the α7 nAChR subunit, and the *Acra7* homozygous mice lacking α7 nAChR channels, all demonstrated considerable down-regulation of terminal differentiation gene expression at the transcriptional and/or translational levels. On the other hand, inhibition of the α7 nAChR pathway favored expression of the cell cycle progression regulators stimulating cell growth and decreased expression of the proapoptotic caspase 3. The α7 nAChR-related changes in the cell cycle and differentiation caused a transient delay in skin development observed in α7 KO mice during the first 3 wk of their lives. These alterations in the genetically determined unfolding of the keratinocyte differentiation program in α7 KO mice and phenotypic abnormalities consistent with delayed epidermal turnover were associated with changes in the repertoire of keratinocyte nAChR subtypes, suggesting that the nicotinergic pathways dominating in the $\alpha7^{-/-}$ keratinocytes are coupled to maintenance of the immature cell phenotype.

Findings of the new and important biological function of "neuronal" α7 nAChR in a nonneuronal location such as the physiologic control of homeostasis and terminal differentiation of the stratified squamous epithelium was anticipated based on the following reasons. First, despite multiple morphological, biochemical, and electrophysiological studies, the functions of neuronal α-BTX binding sites in the mammalian brain remain largely unknown. Furthermore, a mutation deleting the last three exons of the gene for the α7 nAChR subunit that completely eliminates its potential for participation in an ion channel does not alter normal general appearance, growth, survival, gait, anatomy, and baseline behavioral responses (Orr-Urtreger et al., 1997; Paylor et al., 1998). Thus, although the *Acra7* homozygous mutant mice demonstrated that the α7 subunit is not essential for normal devel-

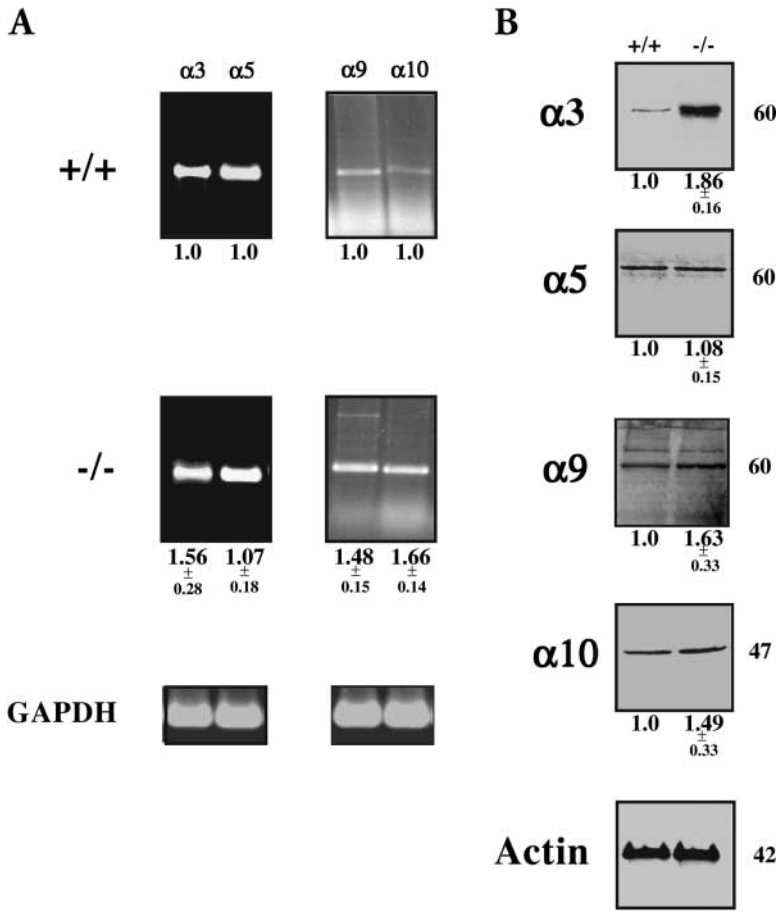

Figure 6. **Alterations in the α3, α5, α9, and α10 nAChR subunit gene expression in α7 KO keratinocytes.** (A) The levels of α3, α5, α9, and α10 nAChR subunit gene transcription in $\alpha7^{-/-}$ keratinocytes. The detection of the nAChR subunit transcripts by RT-PCR was performed using gene specific primers for the murine α3, α5, α9, and α10 nAChR subunits (Table II) and cDNA from the second passage, ~75% confluent monolayers of neonatal α7 homozygous null (−/−) and wild-type (+/+) mice as template. Each pair of primers yielded a PCR product of the expected size: 485 bp for α3, 480 bp for α5, 458 bp for α9, and 463 bp for α10. (B) The levels of α3, α5, α9, and α10 nAChR subunit gene translation in $\alpha7^{-/-}$ keratinocytes. The nAChR subunit proteins were visualized by Western blots of total proteins extracted from the same cells as in A. Results of a representative experiment showing protein bands recognized by rabbit polyclonal antibodies specific for α3, α5, α9, or α10 (Table III) resolved on 15% SDS-PAGE and immunoblotted as described in Materials and methods. The apparent mol wt of each receptor protein is shown in kD at the right side of the gel.

opment or for apparently normal neurological function, they proved to have phenotypic abnormalities in the epidermis, thus providing a valuable tool for defining the functional role of the keratinocyte α7 nAChR channel in the epidermis.

Second, in addition to modulation of neurotransmitter release the α7 nAChR has been implicated in regulating neuronal growth and differentiation via a large variety of genomic and nongenomic effects, including the promotion of neuronal proliferation (Quik et al., 1994; Plummer et al., 2000), neuroprotection (Gueorguiev et al., 2000; Li et al., 2000; Garrido et al., 2001), and induction of apoptosis (Renshaw et al., 1993; Hory-Lee and Frank, 1995; Berger et al., 1998). Neuronal α7 nAChR acts through different intracellular transduction pathways to protect or kill cells (Li et al., 1999). It has been proposed that α7 nAChR helps regulate neuronal development by modulating intracellular Ca^{2+} levels and thus affecting neuronal differentiation and synaptogenesis (Broide and Leslie, 1999). The genomic effects downstream of α7 nAChR are represented by activation of tyrosine hydroxylase and dopamine β-hydroxylase gene expression in PC12 cells (Gueorguiev et al., 2000), whereas the nongenomic pathways involve regulation of protein phosphorylation (Schuller et al., 2000; Kihara et al., 2001).

Third, the α7 subunit is abundantly expressed in the epithelial cells lining skin, oral mucosa, esophagus, trachea, and bronchi, in which nicotinergic stimulation alters cellular metabolism of Ca^{2+} (Grando et al., 1996; Zia et al., 1997; Nguyen et al., 2000a), endothelial cells (Wang et al., 2001), and in cells surrounding large airways and blood vessels, alveolar type II cells, free alveolar macrophages, and pulmonary neuroendocrine cells (Sekhon et al., 1999). In the mammalian fetal lung, α7 nAChR may regulate neuropeptide release, collagen expression, and ultimately lung development (Sekhon et al., 1999). The expression of α7 nAChR channels on the cell membrane of nonneuronal cells is modulated by exposure to Nic (Zia et al., 1997; Arredondo et al., 2001), which may provide a mechanism for Nic-induced changes in gene expression (Arredondo et al., 2001; Zhang et al., 2001a,b), proliferation (Waggoner and Wang, 1994; Stone et al., 2001), apoptosis (LeSage et al., 1999; Heeschen et al., 2001), secretion (LeSage et al., 1999), and tumor growth (Heeschen et al., 2001) in nonneuronal locations.

The contribution of different nAChR subunits to formation of ACh-gated nicotinic ion channels in the plasma membrane of keratinocytes changes with keratinocyte maturation (Zia et al., 2000). Antibody mapping studies in human epidermis have shown that the bulk of α7 immunoreactivity is localized to the cell membranes of mature keratinocytes comprising the granular layer (Nguyen et al., 2001). In keratinocyte cultures, the abundant expression of α7 was observed on the cell membrane of mature cells, which required preincubation of cultures in KGM containing a differentiation-inducing concentration of Ca^{2+} or Nic (Zia et al., 2000). In contrast, the α3-containing nAChRs are present at the earliest stages of keratinocyte development (Nguyen et al., 2000a; Zia et al., 2000). Extracellular Ca^{2+} has been shown to regulate responses of both α3- and α7-containing nAChRs on chick ciliary ganglion neurons (Liu and Berg, 1999). Al-

though both α3 and α7 subunits can contribute to the nAChRs that are permeable to Ca^{2+}, the ACh-gated ion channels composed of the α7 subunits have the greatest Ca^{2+} permeability (Seguela et al., 1993). The results of this study demonstrated that the need to preincubate keratinocytes at differentiation-inducing concentrations of extracellular Ca^{2+} in order to increase the sensitivity of their response to Nic to a blockage with α-BTX in the $^{45}Ca^{2+}$ influx assay is explained by up-regulated expression of α7 nAChRs.

Results of this study demonstrate that ACh signaling through α7 nAChR channels controls the maturation and the cornification stages of keratinocyte development in the epidermis. Downstream signaling from α7 nAChR regulates expression of cell cycle progression, apoptosis, and terminal differentiation regulators at the transcriptional and/or translational levels. These effects may be mediated, at least in part, by changes in Ca^{2+} metabolism. A "gain of function" mutation of the ACh-gated ion channels comprised by α7 subunits demonstrated that neurons expressing only mutant nAChRs are susceptible to abnormal apoptosis and degeneration, possibly due to increased Ca^{2+} influx (Treinin and Chalfie, 1995; Orr-Urtreger et al., 2000; Broide et al., 2001). We found that neither α-BTX could completely block Nic-induced differential of keratinocytes nor anti-α7 AsOs could completely abolish the process of cornification elicited by increasing the concentration of extracellular Ca^{2+} in KGM. Instead of using Nic to induce keratinocytes differentiation as in experiments with α-BTX, the differentiation of anti-α7 AsOs-treated keratinocytes was induced through alternative pathway(s) sensitive to high extracellular Ca^{2+}, since in these cells the α7 nAChR pathway was inactivated due to treatment with anti-α7 AsOs. These findings suggest that the α7 nAChR-mediated pathway works together with other cholinergic and noncholinergic signaling pathways to sustain a constant advancement of a keratinocyte through its differentiation stages toward its programmed death. In acute experiments, such as treatment of cells with α-BTX or anti-α7 AsOs, the alternative pathway apparently could not get engaged fast enough to compensate for the missing function, which is illustrated by an approximately fivefold drop in the number of cells capable of spontaneous cornified envelope formation (Fig. 1). In marked contrast, in the epidermis of α7 KO mice the process of cornification, although delayed, proceeds via a normal path, surfacing skin of these mice with an impermeable barrier or the stratum corneum. Therefore, a lesser magnitude of changes of the gene expression in keratinocytes residing in the epidermis of α7 KO mice (Fig. 4 E) compared with keratinocytes treated with anti-α7 AsOs (Fig. 3 C), as judged from the results of the Western blotting assay, may be explained by putative physiologic backup mechanisms activated during the development of a KO mouse but lacking in the cells treated with AsOs in which the α7 AChRs are inactivated acutely at the posttranscriptional level.

To test a hypothesis that mutational deletion of α7 brings about changes in the repertoire of nAChR channels, we determined the ratios of different α subunit gene expression in $\alpha7^{-/-}$ keratinocytes. We found alterations in the expression of α3, α9, and α10 nAChRs subunits, indicating that the nicotinergic signaling in the skin of α7 KO mice is predominantly mediated via a nAChR complex containing α3 without α5 and both homomeric α9- and heteromeric α9α10-made nAChRs. This switch in subunit composition of the nAChR-gated ion channels may, in turn, bring about a corresponding switch in the ionic properties of the ion channels formed because of shifting of the nicotinergic signaling to the nAChRs that differ in subunit composition, pharmacology, conductance, and kinetics and in their permeability to and modulation by Ca^{2+}. For instance, it has been shown that α5 subunit increases Ca^{2+} permeability of α3 nAChR so that the Ca^{2+} permeability of α3β2α5 nAChRs is comparable to that of α7 nAChRs (Gerzanich et al., 1998). Hence, a relative decrease of the proportion of α3 nAChRs containing α5 subunits, i.e., α3β2α5, in $\alpha7^{-/-}$ keratinocytes can bring about corresponding changes in the ionic properties of the channel, leading to a complex changes in cell cycle regulation, including proliferation-inducing effects, DNA repair and replication anomalies, and antiapoptotic gene activation. On the other hand, up-regulated expression of α9-containing nAChRs that mediate proapoptotic action of ACh at the granular cell–corneocyte transition, which culminates in programmed cell death within the epidermis (Nguyen et al., 2001), may compensate for a lacking component of the nicotinergic control of terminal differentiation of $\alpha7^{-/-}$ keratinocytes, allowing formation of the functional epidermal barrier in α7 KO mice. The nAChR incorporating α9 subunits represents a novel ionotropic and metabotropic receptor/Ca^{2+} channel (Elgoyhen et al., 1994; Glowatzki et al., 1995; Wikstrom et al., 1998). Compared with homomeric α9 channels, the α9α10 nAChR channel displays faster and more extensive agonist-mediated desensitization, a distinct current-voltage relationship, and a biphasic response to changes in extracellular Ca^{2+} ions (Elgoyhen et al., 2001). Thus, although the use of KO mice is probably the most straightforward and rewarding approach to dissect biological function of each particular type of keratinocyte nAChRs, providing an unambiguous mechanistic insight into differential control of keratinocyte functions by ACh, the missing function may be partially compensated or obscured due to engagement of the alternative regulatory pathways.

In conclusion, the comprehensive analysis of the biological role of α7 nAChR in keratinocytes revealed its important role in sustaining normal unfolding of the genetically determined program of cell differentiation eventuating in cell death, or cornification, which is required for formation of the skin barrier. The ACh signaling through α7-made channels may evoke rapid and profound changes in the cellular metabolism of free Ca^{2+} due to modulation of its transmembrane flux. The downstream signaling apparently harbor both genomic and nongenomic effects, the biologic sum of which determines the rate of keratinocyte progression through the differential steps. In *Acra7* homozygous mutant mice, the missing regulatory pathway causes transient changes in skin phenotype characteristic of delayed epidermal turnover. The changes are partially compensated due to redirection of the nicotinergic signaling via the α3-type keratinocyte nAChRs that in the past were found to be associated with immature cell phenotype (Zia et al., 2000), and the α9-type keratinocyte nAChRs that are coupled to regulation of keratinocyte apoptotic secretion (Nguyen et al., 2001).

Materials and methods

Human keratinocyte culture experiments

Human keratinocyte cultures were started from normal neonatal foreskins as we described in detail earlier (Grando et al., 1993a). The cells were grown in 75-cm^2 flasks (Corning Glass Works) in KGM containing 0.09 mM Ca^{2+} (GIBCO BRL) at 37°C in a humid 5% CO_2 incubator. To study nicotinergic effect on cell differentiation, keratinocytes were seeded into 6-well tissue culture plates (Falcon 3046; Becton Dickinson) at a cell density of 10^5/well, grown to ~75% confluence in 2 ml of KGM containing 0.09 mM Ca^{2+}, after which the monolayers received KGM containing 10 μM Nic, 10 μM Nic plus 1 μM α-BTX (both from Sigma-Aldrich), or no additions (control), and the incubation was continued for additional periods of time (as described in Results) with replacing KGM every other day. After incubation, the monolayers were washed with prewarmed Ca^{2+}- and Mg^{2+}-free PBS (GIBCO BRL) and used either in immunocytochemical assay of differentiation marker expression (see below) or in a modification of the spontaneous cornified envelope formation assay (Rice and Green, 1979) as described in detail elsewhere (Grando et al., 1996).

α7 KO mice and murine keratinocyte cultures

The α7 KO mice used in experiments were *Acra7*-deficient (α7 null) mice generated as described previously (Orr-Urtreger et al., 1997). All control mice were $\alpha7^{+/+}$ littermates of $\alpha7^{+/-}$ mice. The animals were killed, and skin samples were collected. The samples destined to RNA and protein extractions were fresh-frozen in liquid nitrogen or freshly embedded in the OCT Tissue Tek compound (Sakura) for use in IF experiments. All of the experiments were conducted by an experimenter that was blind to the genotype of the mice. The genotyping was performed by PCR and Southern analysis as detailed elsewhere (Orr-Urtreger et al., 1997). Cell cultures were grown at 37°C and 5% CO_2 in 25 cm^2 Falcon culture flasks using the cell culture techniques optimized for mouse keratinocytes (Li et al., 1995; Lee et al., 1997).

Immunocytochemical assay

Immunocytochemical analysis of nicotinergic effects on the expression of differentiation markers was performed in situ in keratinocyte monolayers as described previously (Grando et al., 1996). Stained monolayers were examined microscopically and photographed. The numbers of cytokeratin 10–, transglutaminase-, involucrin-, and filaggrin-positive cells were counted in at least three different microscopic fields at the magnification ×200, and the results were expressed as a percentage of the total cells. At least 50 cell per each microscopic field were examined.

IF assay

The IF experiments with skin samples of $\alpha7^{-/-}$ and $\alpha7^{+/+}$ mice were performed as detailed previously (Ndoye et al., 1998) using a computer-assisted image analysis with a software package purchased from Scanalytics. The intensity of fluorescence was calculated pixel by pixel by dividing the summation of the fluorescence intensity of all pixels by the area occupied by the pixels (i.e., segment) and then subtracting the mean intensity of fluorescence of a tissue-free segment (i.e., background).

$^{45}Ca^{2+}$ influx assay

The experiments were performed in triplicate samples according to our modification (Zia et al., 2000) of standard protocols (De Aizpurua et al., 1988). Briefly, freshly isolated human neonatal foreskin keratinocytes were counted with a hemocytometer and aliquoted in incubation buffers at a concentration of 3×10^6 cells per 50 μl per each Eppendorf tube. To measure basal and nicotinergic $^{45}Ca^{2+}$ influx, we used Krebs buffer (Sigma-Aldrich) supplemented to contain 1.2 mM Ca^{2+} ("basal" buffer; pH 7.4). Cell aliquots were resuspended in 300 μl of basal buffer containing test nicotinergic agents and $^{45}Ca^{2+}$ (specific activity 11.6 mCi/mmol; NEN) 1% of total Ca^{2+}, and incubated for 1 min at 37°C. After washing three times by centrifugation at 250 *g* for 1 min in a Beckman Coulter microcentrifuge in ice-cold, radioactive calcium-free basal buffer, the cells were solubilized in 100 μl Triton X-100 (Sigma-Aldrich), transferred into scintillation vials containing 5.0 ml of a scintillation cocktail, and $^{45}Ca^{2+}$ taken up by the cells was measured in a liquid scintillation counter. The amount of the ligand-dependent $^{45}Ca^{2+}$ influx was expressed as a percentage of basal influx.

AsOs assay

The phosphorothioated and FITC-tagged AsOs and the phosphorothioated, equally sized sense oligonucleotide (control) were commercially synthesized by Operon. Following the protocol provided by the manufacturer, AsOs were mixed with LipofectAMINE PLUS™ reagent (GIBCO BRL) and transfected into second passage human foreskin keratinocytes grown to ~50% confluence in a standard 6-well tissue culture plate in 2.0 ml KGM. Each experimental culture received 20 nM of AsOs, and the control cultures received the same dose of control (sense) oligonucleotide, diluted in KGM containing 1.2 mM Ca^{2+}, to induce keratinocyte differentiation (Hennings and Holbrook, 1983).

α7 nAChR expression assays

To assess the effects of changes in extracellular Ca^{2+} concentrations on the expression of keratinocyte α7 nAChRs, keratinocytes freshly isolated from human neonatal foreskins were incubated for 0, 15, or 60 min in KGM containing 1.2 mM Ca^{2+} in a humid 5% CO_2 incubator after which the to-

Table III. **The primary antibodies used in IF assays**

Antibody specificity	Isotype	Host	Concentration	Epitope	Reactivity
			μg/ml		
nAChRa3[a]	IgG	Rabbit	1	CPLMAREDA	Human and rodent
nAChRa5[a]	IgG	Rabbit	1	CPVHIGNANK	Human and rodent
nAChRa7[a]	IgG	Rabbit	1	CFVEAVSKDFA	Human and rodent
nAChRa9[b]	IgG	Rabbit	1	CWHDAYLTWDRDQYDRLD and CNKADDESSEPVNTN	Human and rodent
nAChRa10[c]	IgG	Rabbit	1	RSHRAAQRRHEDWKR	Human and rodent
p53[d]	IgG1	Rabbit	5	RHSVV	Human and rodent
Cyclin D1[d]	IgG2	Rabbit	1	1–295 (whole protein)	Human and rodent
PCNA[d]	IgG2	Rabbit	2.5	1–261 (whole protein)	Human and rodent
Bcl-2[d]	IgG	Rabbit	0.5	20–30 aa	Human and rodent
Caspase 3[d]	IgG	Rabbit	1	whole protein	Human and rodent
CK 1[e]	IgG	Rabbit	0.4	SSVKFCSTTYSGVTRC	Human and rodent
CK 10[e]	IgG	Rabbit	1	SGTGGGDQSSKGPNY	Human and rodent
Filaggrin[e]	IgG	Rabbit	0.5	DSQVHSGVQVEGRRGH	Human and rodent
β-Actin[f]	IgG1	Mouse	0.2	PPIAALVIPSGSGL	Human and rodent
Ki-67[g]	IgG1	Rabbit	1	2,597–2,896	Human and rodent

[a]Research and Diagnostic Antibodies.
[b]Raised and characterized as detailed in Nguyen et al. (2000b).
[c]The antiserum was raised against a 15 amino acid residue peptide (NH_2-RSHRAAQRRHEDWKR-$CONH_2$) identical to aa 404–417 of the predicted α10 protein (Elgoyhen et al., 2001). Preimmune serum was isolated. After this, a rabbit received injections of the peptide at 14-d intervals (total of five injections; Pineda Antikörper-Service). Standard procedures were used to further characterize the antibody.
[d]Oncogene Research Products.
[e]BabCo.
[f]Sigma-Aldrich.
[g]Santa Cruz Biotechnology, Inc.

tal amount of α7 protein was measured by Western blotting (as described below), and the membrane expression of this nAChR was evaluated using FITC-labeled α-BTX (Garcia-Borron et al., 1990). Briefly, quadruplicate of experimental, i.e., 1.2 mM Ca^{2+}-treated, and control, i.e., 0.09 mM Ca^{2+}-treated, keratinocytes were resuspended in ice-cold PBS containing 10 μM FITC-labeled α-BTX (Molecular Probes, Inc.), incubated for 1 h at 4°C, washed three times with PBS, loaded in standard 96-well ELISA plates (Costar Corporation) at a concentration of 5×10^4/well, and the fluorescence intensity ratio (at 494 nm excitation and 518-nm emission wavelengths) was measured using the Perkin Elmer HTS 7000 instrument.

Western blot assay

Proteins were isolated from the phenol-ethanol supernatant of homogenized human or murine keratinocytes or skin samples of neonatal mice by adding 1.5 ml of isopropyl alcohol per 1 ml of Trizol Reagent (GIBCO BRL) and analyzed essentially as described in our protocol of a quantitative immunoblot assay (Arredondo et al., 2001). The specificities and working concentrations of primary antibodies used are listed in Table III. The membranes were developed using the ECL + Plus chemiluminescent detection system (Amersham Biosciences). To visualize antibody binding, the membranes were scanned with Storm™/FluorImager (Molecular Dynamics), and band intensities were determined by area integration using ImageQuant software (Molecular Dynamics). To normalize for the protein content, the housekeeping protein actin was visualized in each sample with a mouse antiactin monoclonal antibody (Sigma-Aldrich). The ratios obtained in three independent experiments were averaged to obtain the mean value ($n = 3$). The protein content ratio in every control (or $\alpha7^{+/+}$) sample is always equal to 1. The images represent typical results from a series of three independent experiments.

RT-PCR assay

Total RNA was extracted from cultured keratinocytes and murine skin using guanidinium thiocyanate phenol chloroform extraction procedure (Trizol Reagent; GIBCO BRL) as described elsewhere (Chomczynski and Sacchi, 1987). 1 μg of dried, DNase-treated RNA was reverse transcribed in 20 μl of RT-PCR mix (50 mM Tris, pH 8.3, 6 mM $MgCl_2$, 40 mM KCl, 25 mM dNTPs, 1 μg Oligo-dt [GIBCO BRL], 1 mM DTT, 1 U RNase inhibitor [Boehringer] and 10 U SuperScript II [GIBCO BRL]) at 42°C for 2 h. The PCR was performed in a final volume of 50 μl containing 1 μl of the single strand cDNA product, 10 mM Tris-HCl (pH 9.0), 5 mM KCl, 5 mM $MgCl_2$, 0.2 mM dATP, 0.2 mM dCTP, 0.2 mM dGTP, 0.2 mM dTTP, and 2.5 U Taq DNA polymerase (Perkin Elmer) and 20 pmol of each forward (5′) and reverse (3′) primers. To allow a quantitative determination of relative gene expression levels (Arredondo et al., 2001), the cDNA content of the samples was normalized, and the linear range of amplification was determined for each primer set. For each experiment, the housekeeping gene GAPDH was amplified with 20–30 cycles to normalize the cDNA content of the samples. The amplification was performed at 94°C (1 min), 60°C (2 min), and 72°C (3 min) for 24–30 cycles. The specific primers used in this study are shown in Table II. The reported ratios derived from the combination of the data obtained in three independent experiments ($n = 3$). The images represent typical results from a series of three independent experiments. To standardize the analysis, the gene expression ratio in the control (or $\alpha7^{+/+}$) sample is always equal to 1.

Statistics

The results of the quantitative assays were expressed as mean ± SD. Significance was determined using Student's *t* test.

We thank Dr. Arthur L. Beaudet (Baylor College of Medicine, Houston, Texas) for making α7 KO mice available for experiments reported in this paper and for providing strong intellectual support throughout the study. We are also grateful to Arlene D. Gonzales (Biology & Biotechnology Research Program, Lawrence Livermore National Laboratory, Livermore, California) for help with experiments with antisense oligonucleotides. We thank Tamara E. Rees for her help with illustrations.

This work was supported by National Institutes of Health grants DE14173 and GM62136 and research grants from the Unilever Research-USA and Flight Attendant Medical Research Institute to S.A. Grando, and the grant SFB 547, project C2 to W. Kummer.

Submitted: 21 June 2002
Revised: 3 September 2002
Accepted: 3 September 2002

References

Arredondo, J., V.T. Nguyen, A.I. Chernyavsky, D.L. Jolkovsky, K.E. Pinkerton, and S.A. Grando. 2001. A receptor-mediated mechanism of nicotine toxicity in oral keratinocytes. *Lab. Invest.* 81:1653–1668.

Berger, F., F.H. Gage, and S. Vijayaraghavan. 1998. Nicotinic receptor-induced apoptotic cell death of hippocampal progenitor cells. *J. Neurosci.* 18:6871–6881.

Broide, R.S., and F.M. Leslie. 1999. The α7 nicotinic acetylcholine receptor in neuronal plasticity. *Mol. Neurobiol.* 20:1–16.

Broide, R.S., A. Orr-Urtreger, and J.W. Patrick. 2001. Normal apoptosis levels in mice expressing one α7 nicotinic receptor null and one L250T mutant allele. *Neuroreport.* 12:1643–1648.

Chomczynski, P., and N. Sacchi. 1987. Single-step method of RNA isolation by acid guanidinium thiocyanate-phenol-chloroform extraction. *Anal. Biochem.* 162:156–159.

De Aizpurua, H.J., E.H. Lambert, G.E. Griesmann, B.M. Olivera, and V.A. Lennon. 1988. Antagonism of voltage-gated calcium channels in small cell carcinomas of patients with and without Lambert-Eaton myasthenic syndrome by autoantibodies omega-conotoxin and adenosine. *Cancer Res.* 48:4719–4724.

Elgoyhen, A.B., D.S. Johnson, J. Boulter, D.E. Vetter, and S. Heinemann. 1994. α9: an acetylcholine receptor with novel pharmacological properties expressed in rat cochlear hair cells. *Cell.* 79:705–715.

Elgoyhen, A.B., D.E. Vetter, E. Katz, C.V. Rothlin, S.F. Heinemann, and J. Boulter. 2001. α10: a determinant of nicotinic cholinergic receptor function in mammalian vestibular and cochlear mechanosensory hair cells. *Proc. Natl. Acad. Sci. USA.* 98:3501–3506.

Foley, J., B.J. Longely, J.J. Wysolmerski, B.E. Dreyer, A.E. Broadus, and W.M. Philbrick. 1998. PTHrP regulates epidermal differentiation in adult mice. *J. Invest. Dermatol.* 111:1122–1128.

Garcia-Borron, J.C., M.A. Chinchetru, and M. Martinez-Carrion. 1990. Selective labeling of α-bungarotoxin with fluorescein isothiocyanate and its use for the study of toxin-acetylcholine receptor interactions. *J. Protein Chem.* 9:683–693.

Garrido, R., M.P. Mattson, B. Hennig, and M. Toborek. 2001. Nicotine protects against arachidonic-acid-induced caspase activation, cytochrome c release and apoptosis of cultured spinal cord neurons. *J. Neurochem.* 76:1395–1403.

Gerzanich, V., F. Wang, A. Kuryatov, and J. Lindstrom. 1998. α5 subunit alters desensitization, pharmacology, Ca^{++} permeability and Ca^{++} modulation of human neuronal α3 nicotinic receptors. *J. Pharmacol. Exp. Ther.* 286:311–320.

Gibbs, S., A.N.S. Pinto, S. Murli, M. Huber, D. Hohl, and M. Ponec. 2000. Epidermal growth factor and keratinocyte growth factor differentially regulate epidermal migration, growth, and differentiation. *Wound Repair Regen.* 8:192–203.

Glowatzki, E., K. Wild, U. Braendle, G. Fakler, B. Fakler, H.P. Zenner, and J.P. Ruppersberg. 1995. Cell-specific expression of the α9 nACh receptor subunit in auditory hair cells revealed by single-cell RT-PCR. *Proc. R Soc. Lond. B Biol. Sci.* 262:141–147.

Grando, S.A. 1997. Biological functions of keratinocyte cholinergic receptors. *J. Investig. Dermatol. Symp. Proc.* 2:41–48.

Grando, S.A. 2001. Receptor-mediated action of nicotine in human skin. *Int. J. Dermatol.* 40:691–693.

Grando, S.A., R. Cabrera, B.S. Hostager, P.L. Bigliardi, J.S. Blake, M.J. Herron, M.V. Dahl, and R.D. Nelson. 1993a. Computerized microassay of keratinocyte cell-plastic attachment and proliferation for assessing net stimulatory inhibitory and toxic effects of compounds on nonimmortalized cell lines. *Skin Pharmacol.* 6:135–147.

Grando, S.A., D.A. Kist, M. Qi, and M.V. Dahl. 1993b. Human keratinocytes synthesize, secrete and degrade acetylcholine. *J. Invest. Dermatol.* 101:32–36.

Grando, S.A., R.M. Horton, T.M. Mauro, D.A. Kist, T.X. Lee, and M.V. Dahl. 1996. Activation of keratinocyte nicotinic cholinergic receptors stimulates calcium influx and enhances cell differentiation. *J. Invest. Dermatol.* 107: 412–418.

Grando, S.A., R.M. Horton, E.F.R. Pereira, B.M. Diethelm-Okita, P.M. George, E.X. Albuquerque, and B.M. Conti-Fine. 1995. A nicotinic acetylcholine receptor regulating cell adhesion and motility is expressed in human keratinocytes. *J. Invest. Dermatol.* 105:774–781.

Gueorguiev, V.D., R.J. Zeman, E.M. Meyer, and E.L. Sabban. 2000. Involvement of α7 nicotinic acetylcholine receptors in activation of tyrosine hydroxylase and dopamine β-hydroxylase gene expression in PC12 cells. *J. Neurochem.* 75:1997–2005.

Heeschen, C., J.J. Jang, M. Weis, A. Pathak, S. Kaji, R.S. Hu, P.S. Tsao, F.L. Johnson, and J.P. Cooke. 2001. Nicotine stimulates angiogenesis and pro-

motes tumor growth and atherosclerosis. *Nat. Med.* 7:833–839.

Hennings, H., and K.A. Holbrook. 1983. Calcium regulation of cell-cell contact and differentiation of epidermal cells in culture. An ultrastructural study. *Exp. Cell Res.* 143:127–142.

Hory-Lee, F., and E. Frank. 1995. The nicotinic blocking agents d-tubocurare and α-bungarotoxin save motoneurons from naturally occurring death in the absence of neuromuscular blockade. *J. Neurosci.* 15:6453–6460.

Kihara, T., S. Shimohama, H. Sawada, K. Honda, T. Nakamizo, H. Shibasaki, T. Kume, and A. Akaike. 2001. α7 nicotinic receptor transduces signals to phosphatidylinositol 3-kinase to block A β-amyloid-induced neurotoxicity. *J. Biol. Chem.* 276:13541–13546.

Lee, Y.S., A.A. Dlugosz, R. McKay, N.M. Dean, and S.H. Yuspa. 1997. Definition by specific antisense oligonucleotides of a role for protein kinase C alpha in expression of differentiation markers in normal and neoplastic mouse epidermal keratinocytes. *Mol. Carcinog.* 18:44–53.

LeSage, G., D. Alvaro, A. Benedetti, S. Glaser, L. Marucci, L. Baiocchi, W. Eisel, A. Caligiuri, J.L. Phinizy, R. Rodgers, et al. 1999. Cholinergic system modulates growth, apoptosis, and secretion of cholangiocytes from bile duct-ligated rats. *Gastroenterology.* 117:191–199.

Levandoski, M.M., Y. Lin, L. Moise, J.T. McLaughlin, E. Cooper, and E. Hawrot. 1999. Chimeric analysis of a neuronal nicotinic acetylcholine receptor reveals amino acids conferring sensitivity to alpha-bungarotoxin. *J. Biol. Chem.* 274:26113–26119.

Li, L., R.W. Tucker, H. Hennings, and S.H. Yuspa. 1995. Chelation of intracellular Ca^{2+} inhibits murine keratinocyte differentiation *in vitro*. *J. Cell. Physiol.* 163:105–114.

Li, Y., R.L. Papke, Y.J. He, W.J. Millard, and E.M. Meyer. 1999. Characterization of the neuroprotective and toxic effects of α7 nicotinic receptor activation in PC12 cells. *Brain Res.* 830:218–225.

Li, Y., M.A. King, and E.M. Meyer. 2000. α7 nicotinic receptor-mediated protection against ethanol-induced oxidative stress and cytotoxicity in PC12 cells. *Brain Res.* 861:165–167.

Lindstrom, J. 1997. Nicotinic acetylcholine receptors in health and disease. *Mol. Neurobiol.* 15:193–222.

Liu, Q.S., and D.K. Berg. 1999. Extracellular calcium regulates responses of both α3- and α7-containing nicotinic receptors on chick ciliary ganglion neurons. *J. Neurophysiol.* 82:1124–1132.

Ndoye, A., R. Buchli, B. Greenberg, V.T. Nguyen, S. Zia, J.G. Rodriguez, R.J. Webber, M.A. Lawry, and S.A. Grando. 1998. Identification and mapping of keratinocyte muscarinic acetylcholine receptor subtypes in human epidermis. *J. Invest. Dermatol.* 111:410–416.

Nguyen, V.T., L.L. Hall, G. Gallacher, A. Ndoye, D.L. Jolkovsky, R.J. Webber, R. Buchli, and S.A. Grando. 2000a. Choline acetyltransferase, acetylcholinesterase, and nicotinic acetylcholine receptors of human gingival and esophageal epithelia. *J. Dent. Res.* 79:939–949.

Nguyen, V.T., A. Ndoye, and S.A. Grando. 2000b. Novel human α9 acetylcholine receptor regulating keratinocyte adhesion is targeted by pemphigus vulgaris autoimmunity. *Am. J. Pathol.* 157:1377–1391.

Nguyen, V.T., A. Ndoye, L.L. Hall, S. Zia, J. Arredondo, A.I. Chernyavsky, D.A. Kist, B.D. Zelickson, M.A. Lawry, and S.A. Grando. 2001. Programmed cell death of keratinocytes culminates in apoptotic secretion of a humectant upon secretagogue action of acetylcholine. *J. Cell Sci.* 114:1189–1204.

Orr-Urtreger, A., F.M. Goldner, M. Saeki, I. Lorenzo, L. Goldberg, M. De Biasi, J.A. Dani, J.W. Patrick, and A.L. Beaudet. 1997. Mice deficient in the α7 neuronal nicotinic acetylcholine receptor lack α-bungarotoxin binding sites and hippocampal fast nicotinic currents. *J. Neurosci.* 17:9165–9171.

Orr-Urtreger, A., R.S. Broide, M.R. Kasten, H. Dang, J.A. Dani, A.L. Beaudet, and J.W. Patrick. 2000. Mice homozygous for the L250T mutation in the α7 nicotinic acetylcholine receptor show increased neuronal apoptosis and die within 1 day of birth. *J. Neurochem.* 74:2154–2166.

Paylor, R., M. Nguyen, J.N. Crawley, J. Patrick, A. Beaudet, and A. Orr-Urtreger. 1998. α7 nicotinic receptor subunits are not necessary for hippocampal-dependent learning or sensorimotor gating: a behavioral characterization of *Acra7*-deficient mice. *Learn. Mem.* 5:302–316.

Plummer, H.K., III, B.J. Sheppard, and H.M. Schuller. 2000. Interaction of tobacco-specific toxicants with nicotinic cholinergic regulation of fetal pulmonary neuroendocrine cells: implications for pediatric lung disease. *Exp. Lung Res.* 26:121–135.

Quik, M., J. Chan, and J. Patrick. 1994. α-Bungarotoxin blocks the nicotinic receptor mediated increase in cell number in a neuroendocrine cell line. *Brain Res.* 655:161–167.

Renshaw, G., P. Rigby, G. Self, A. Lamb, and R. Goldie. 1993. Exogenously administered α-bungarotoxin binds to embryonic chick spinal cord: implications for the toxin-induced arrest of naturally occurring motoneuron death. *Neuroscience.* 53:1163–1172.

Rice, R.H., and H. Green. 1979. Presence in human epidermal cells of a soluble protein precursor of the cross-linked envelope: activation of the cross-linking by calcium ions. *Cell.* 18:681–694.

Schuller, H.M., B.A. Jull, B.J. Sheppard, and H.K. Plummer. 2000. Interaction of tobacco-specific toxicants with the neuronal α7 nicotinic acetylcholine receptor and its associated mitogenic signal transduction pathway: potential role in lung carcinogenesis and pediatric lung disorders. *Eur. J. Pharmacol.* 393:265–277.

Seguela, P., J. Wadiche, K. Dineley-Miller, J.A. Dani, and J.W. Patrick. 1993. Molecular cloning, functional properties, and distribution of rat brain α7: a nicotinic cation channel highly permeable to calcium. *J. Neurosci.* 13:596–604.

Sekhon, H.S., Y. Jia, R. Raab, A. Kuryatov, J.F. Pankow, J.A. Whitsett, J. Lindstrom, and E.R. Spindel. 1999. Prenatal nicotine increases pulmonary α7 nicotinic receptor expression and alters fetal lung development in monkeys. *J. Clin. Invest.* 103:637–647.

Sgard, F., E. Charpantier, S. Bertrand, N. Walker, D. Caput, D. Graham, D. Bertrand, and F. Besnard. 2002. A novel human nicotinic receptor subunit, α10, that confers functionality to the α9-subunit. *Mol. Pharmacol.* 61:150–159.

Steinbach, J.H. 1990. Mechanism of action of the nicotinic acetylcholine receptor. *In* The Biology Of Nicotine Dependence. Vol. 152. G. Bock and J. Marsh, editors. John Wiley and Sons Ltd., New York. 53–61.

Stone, R.A., R. Sugimoto, A.S. Gill, J. Liu, C. Capehart, and J.M. Lindstrom. 2001. Effects of nicotinic antagonists on ocular growth and experimental myopia. *Invest. Ophthalmol. Vis. Sci.* 42:557–565.

Treinin, M., and M. Chalfie. 1995. A mutated acetylcholine receptor subunit causes neuronal degeneration in *C. elegans*. *Neuron.* 14:871–877.

Waggoner, S.E., and X. Wang. 1994. Effect of nicotine on proliferation of normal, malignant, and human papillomavirus-transformed human cervical cells. *Gynecol. Oncol.* 55:91–95.

Wang, Y., E.F. Pereira, A.D. Maus, N.S. Ostlie, D. Navaneetham, S. Lei, E.X. Albuquerque, and B.M. Conti-Fine. 2001. Human branchial epithelial and endothelial cells express alpha7 nicotinic acetylcholine receptors. *Mol. Pharmacol.* 60:1201–1209.

Wessler, I., C.J. Kirkpatrick, and K. Racke. 1998. Non-neuronal acetylcholine, a locally acting molecule, widely distributed in biological systems: expression and function in humans. *Pharmacol. Ther.* 77:59–79.

Wessler, I., C.J. Kirkpatrick, and K. Racke. 1999. The cholinergic 'pitfall': acetylcholine, a universal cell molecule in biological systems, including humans. *Clin. Exp. Pharmacol. Physiol.* 26:198–205.

Wikstrom, M.A., G. Lawoko, and E. Heilbronn. 1998. Cholinergic modulation of extracellular ATP-induced cytoplasmic calcium concentrations in cochlear outer hair cells. *J. Physiol. (Paris).* 92:345–349.

Zhang, S., I.N. Day, and S. Ye. 2001a. Microarray analysis of nicotine-induced changes in gene expression in endothelial cells. *Physiol. Genomics.* 5:187–192.

Zhang, S., I. Day, and S. Ye. 2001b. Nicotine induced changes in gene expression by human coronary artery endothelial cells. *Atherosclerosis.* 154:277–283.

Zia, S., A. Ndoye, V.T. Nguyen, and S.A. Grando. 1997. Nicotine enhances expression of the α3, α4, α5, and α7 nicotinic receptors modulating calcium metabolism and regulating adhesion and motility of respiratory epithelial cells. *Res. Commun. Mol. Pathol. Pharmacol.* 97:243–262.

Zia, S., A. Ndoye, T.X. Lee, R.J. Webber, and S.A. Grando. 2000. Receptor-mediated inhibition of keratinocyte migration by nicotine involves modulations of calcium influx and intracellular concentration. *J. Pharmacol. Exp. Ther.* 293:973–981.